# Effects of Dielectric Barriers in Radio-Frequency Atmospheric Glow Discharges

Jianjun J. Shi, Dawei W. Liu, and Michael G. Kong, *Senior Member, IEEE*

*(Invited Paper)*

***Abstract*—This paper reports the effects of introducing dielectric barriers to radio-frequency (RF) atmospheric pressure glow discharges (APGD) that have hitherto employed bare electrodes. The resulting atmospheric RF dielectric barrier discharges (DBD) are experimentally shown to retain their large volume without constriction at very large currents, well above the maximum current at which conventional RF APGD with bare electrodes can maintain their plasma stability. Optical emission spectroscopy is used to demonstrate that larger discharge currents lead to more active plasma chemistry. A complementary computational study is then presented on the dynamics and structures of the RF DBD under different operation conditions. While the RF DBD and conventional RF APGD may present very different electrical signatures in the external circuit, it is shown that their discharge properties, particularly the sheath characteristics, are very similar. Finally, it is demonstrated that thinner dielectric barriers or/and larger excitation frequencies are desirable to maximize the largest permissible discharge current without compromising the plasma stability.**

***Index Terms*—Atmospheric pressure glow discharges (APGD), dielectric barrier discharges (DBD), plasma stability.**

## I. Introduction

ATMOSPHERIC pressure glow discharges (APGD) have recently attracted much attention, largely because they offer a chamberless route to many scientific disciplines, including analytical chemistry [1], nanoscience [2], biology and medicine [3]–[5], space exploration [6], and display technologies [7]. Interest in APGD is also motivated by their scope for new low-temperature plasma physics in a highly collisional regime [8]. Of all atmospheric glow discharges, the radio-frequency (RF) APGD offer the distinct advantage of low breakdown voltage, thus allowing for the use of smaller power supplies and enabling a wider range of applications. Different from atmospheric dielectric barrier discharges (DBD) generated typically at frequencies of 1–500 kHz [9], the RF APGD do not require dielectric barriers for their generation as their glow-to-arc transition is controlled by an electron trapping mechanism facilitated by the rapid oscillation of the applied voltage [10], [11]. In fact, almost all studies of the RF APGD have so far been based on bare metallic electrodes [2], [8], [10]–[16].

It is common that a large-current operation of atmospheric glow discharges results in both a greater risk for plasma instability, including the glow-to-arc transition, and a more active plasma chemistry with generated reactive plasma species achieving higher concentrations. In other words, plasma stability and plasma reactivity can become mutually exclusive. From an application standpoint, the plasma stability is critical to application reliability, whereas the plasma reactivity is central to application efficiency. It is therefore desirable to achieve greater plasma reactivity without compromising the plasma stability. In a very recent study, we proposed computationally that the dielectric barriers are useful for expanding the operation of the RF atmospheric glow discharges into regimes of very high current even though they are not essential for plasma ignition [17]. For future reference, we refer the conventional RF APGD with the naked electrodes to as RF APGD and those with dielectrically insulated electrodes to as RF DBD.

As the original proposal of the RF DBD was based on a theoretical prediction [17], it is important to obtain the experimental confirmation. It is equally important to understand how the physics of the RF DBD may differ from that of the RF APGD and how the operation expansion into high-current regimes can be maximized. In Section II, we first present the experimental evidences of operating the RF DBD at larger discharge current than RF APGD and of their capability of producing higher fluxes of reactive plasma species without compromising the plasma stability. With the advantage of the RF DBD being established, we present a complementary computational study in Section III where the effects of dielectric barriers are investigated and discussed. In addition to the current–voltage ($I$–$V$) characteristics and the dissipated power, this computational approach allows an access to sheath voltage, sheath thickness, and spatial profiles of neutral and charged particles, all of which are currently difficult to measure experimentally. These are used to unravel the underpinning physics of the RF DBD and its difference from that of the conventional RF APGD. Also, we consider in Section III the effects of the excitation frequency as it influences the capacitance of the dielectric barriers. Finally, in Section IV, we summarize our findings with concluding remarks.

Manuscript received September 30, 2006; revised November 16, 2006. This work was supported in part by the Engineering and Physical Sciences Research Council, U.K., and in part by the Department of Health, U.K.

The authors are with Department of Electronic and Electrical Engineering, Loughborough University, Leicestershire LE11 3TU, U.K. (e-mail: m.g.kong@lboro.ac.uk).

Color versions of one or more of the figures in this paper are available online at http://ieeexplore.ieee.org.

Digital Object Identifier 10.1109/TPS.2007.893251

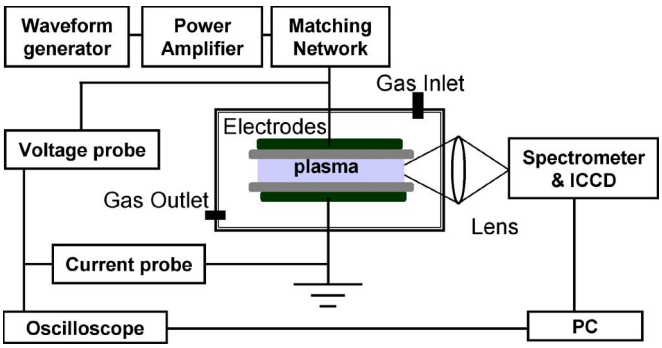


Fig. 1. Schematic of the experimental setup and diagnostics devices.

## II. Experimental Evidence

Our RF APGD system employed two parallel stainless-steel electrodes, one being a round disk of 2 cm in diameter and the other being a rectangular plate of $4 \times 8$ cm$^2$. Hence, the electrode surface area was 3.1 cm$^2$. The two electrodes were naked without any dielectric barriers, and their separation distance was fixed at 2.4 mm. The RF DBD experiments employed exactly the same electrode unit, apart from the two electrodes being dielectrically insulated, each with one ceramic plate of 0.5-mm thick and a relative dielectric constant of $\varepsilon_r = 5.9$. The gas gap was again fixed at 2.4 mm. The electrode unit was housed within a Perspex box fed with a through helium flow at 5 slm. The Perspex box was not airtight, and therefore, the oxygen and nitrogen were present. Fig. 1 shows the schematic of the experimental setup, in which an RF power amplifier (Amplifier Research 150A100B) and a function generator (Tektronix AFG3102) were used to deliver an RF voltage at 6.78 MHz to the electrode unit via a home-made matching network. Current and voltage were measured by a wideband current probe (Tektronix P6021), a wideband voltage probe (Tektronix P6015A), and a digital oscilloscope (Tektronix TDS 3000B). Plasma images were taken with an exposure time of 1 ms using an iCCD camera (Andor i-Star DH720). Optical emission spectrum was measured using a spectrometer system (Andor Shamrock), with a focal length of 0.3 m and a grating of 600 grooves/mm.

For all our experiments, the discharge current was sinusoidal with one positive peak and one negative peak in each RF cycle of the applied voltage. Fig. 2 shows the $I$–$V$ characteristics of the RF DBD and that of its comparable RF APGD with bare electrodes. With the same gas gap, the applied voltage of the RF DBD $V_{\rm a}$ was higher because it was divided onto the gas gap and the two dielectric barriers. At an rms current of 136 mA (or 43.3 mA/cm$^2$), the RF APGD was found to undergo constriction and evolve into a narrow and unstable channel. In the case of the RF DBD on the other hand, the discharge remained stable and diffuse up to 242 mA [or 77.1 mA/cm$^2$ at point (d) in Fig. 2]. It is possible to operate the RF DBD at an even higher discharge current; however, this was limited in our experiments by the power capacity of the RF power amplifier. It is therefore clear that the use of dielectric barriers allows a significant extension of the operation regime of the RF atmospheric glow discharges to large discharge currents. It is worth noting that the $I$–$V_{\rm a}$ relationship of the RF

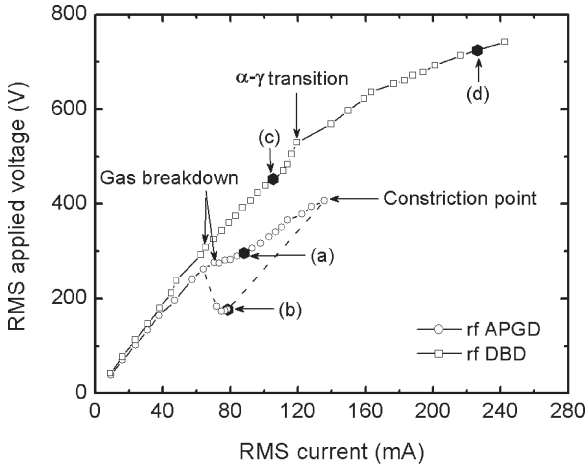


Fig. 2. $I$–$V$ characteristics of an RF DBD in atmospheric helium and that of a comparable RF APGD with bare electrodes. The dashed curve indicates the region where the RF APGD becomes a constricted plasma.

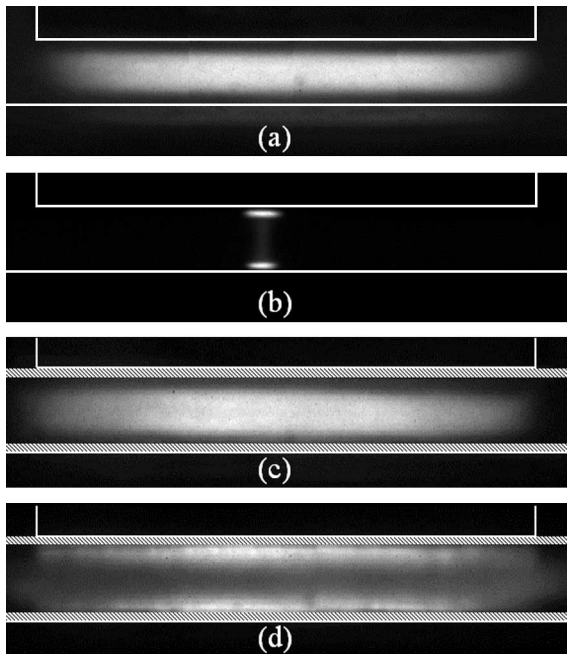


Fig. 3. Images of RF APGD at (a) $I_{\rm rms} = 88$ mA; and (b) 78 mA, and images of RF DBD at (c) 105 mA and (d) 226 mA. These current points correspond to those marked in Fig. 2.

APGD has a positive differential conductivity, and therefore, its operation after the gas breakdown was in the $\alpha$ mode [11], [15], [18] and then evolved into a constricted plasma directly, thus bypassing the $\gamma$ mode. Though the RF DBD also has a positive differential conductivity for $I$–$V_{\rm a}$ relationship, a step change is evident at point (c) around $I_{\rm rms} = 120$ mA. As established previously [17], this step change in the $I$–$V_{\rm a}$ relationship is indicative of the change of the differential conductivity in the $I$–$V_{\rm g}$ relationship from being positive to negative with $V_{\rm g}$ being the gas voltage. Hence, the RF DBD was in the $\alpha$ mode from the gas breakdown to 120 mA and in the $\gamma$ mode from 120 to 242 mA.

Stability of the RF DBD and RF APGD can be demonstrated by plasma images taken at different rms currents. For RF APGD, Fig. 3 shows a uniform and stable discharge at

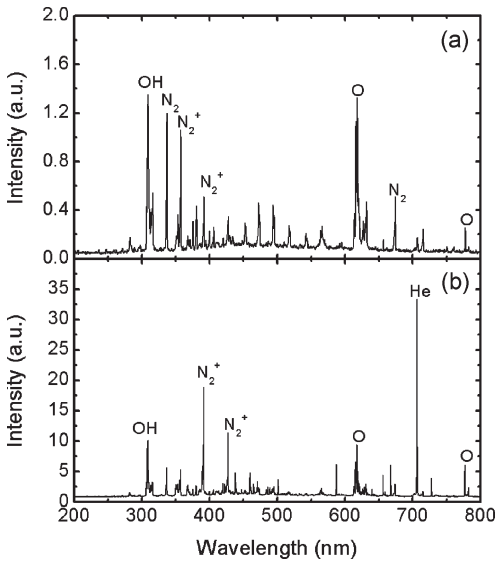


Fig. 4. Optical emission spectra of RF DBD at (a) 105 mA and (b) 226 mA.

$I_{\rm rms} = 88$ mA and an unstable and highly constricted plasma at $I_{\rm rms} = 78$ mA. Plasma constriction is a characteristic of the RF APGD at large discharge currents and responsible for the difficulty of retaining large volume and stability in the $\gamma$ mode. With the dielectric barriers, it becomes much easier to maintain a large-volume RF APGD in both the $\alpha$ mode and the $\gamma$ mode. This is clearly shown in the diffuse and uniform plasma images in Fig. 3(c) and (d), taken at $I_{\rm rms} = 105$ and 226 mA [points (c) and (d) in Fig. 2], respectively. Although not shown, nanosecond imaging was also taken to confirm that plasma images in Fig. 3(a), (c), and (d) were all free of streamers. It is worth noting that the sheath region (as indicated by the dark region near electrodes) in Fig. 3(c) and (d) is narrower at 226 mA than at 105 mA. This is consistent with the simulation results [11], [18].

It is known that active plasma chemistry is more likely to be facilitated at a larger discharge current. To investigate this, we measured the optical emission spectra for the RF DBD at two different discharge currents of $I_{\rm rms} = 105$ and 226 mA. The results are shown in Fig. 4. As the current increases, the atomic oxygen lines at 615 and 777 nm increase by a factor of 8 and 23, respectively, and the hydroxyl (OH) line at 309 nm increases by a factor of 8. Both oxygen atoms and OH radicals are critical for numerous applications such as biological decontamination [19]. Hence, Figs. 3 and 4 confirm the original theoretical prediction [17] that the use of dielectric barriers in RF atmospheric discharges allows for high concentration of reactive plasma species to be achieved without compromising the plasma stability.

## III. Stabilization Mechanisms and Optimization

To understand the mechanisms through which the RF DBD achieve a high plasma stability at large discharge currents, it is useful to study their dynamics and structures. This can be greatly assisted by the dynamics of the sheath structure [8]. However, the current diagnostics tools for the APGD are inadequate for reliable measurement of the sheath electric field, and as a result, we employ a computational approach as an alternative. Our numerical code is based on a fluid model in which the electrons are described in terms of their mean kinetic energy, whereas all heavy particles are treated hydrodynamically with equilibrium with the local electric field [11], [18]. To focus on the main plasma characteristics, we consider pure helium as the background gas and ignore the effects of impurity gases. The numerical model includes six plasma species, namely the electron $e$, helium ion $\mathrm{He}^+$, excited helium atom $\mathrm{He}^*$, dimer helium ion $\mathrm{He}_2^+$, excited dimer atom $\mathrm{He}_2^*$, and background helium atoms He. Relevant reaction mechanisms and transport coefficients are the same as those used in the literature [10], [18], [20]. Rates for reactions involving electrons are expressed in terms of the electron mean energy rather than the local electric field to enable an accurate description of the electrode sheath region [8], [10], [18], [20]. Based on this fluid model, our numerical code has already been shown to agree with the experimental data [11], [18] and is therefore reliable to use as a theoretical tool. For simplicity, we consider the pure helium case only. We have previously established that the key stabilization mechanism in the RF DBD is the current-limiting ability of the dielectric barriers, particularly at large applied voltage [17]. While this current-limiting ability is achieved in the external circuit by dividing into the applied voltage, it is less clear whether the discharge characteristics may be affected by the presence of the dielectric barriers. To this end, we study how the RF DBD characteristics may change when the thickness of the dielectric barriers or the excitation frequency is altered.

### A. *Effects of the Barrier Thickness*

Fig. 5(a) shows the discharge current dependence of the applied and gas voltages for three different thicknesses of dielectric barriers and at the same excitation frequency of 13.56 MHz. At any given current density, thicker dielectric barriers are seen to lead to higher applied voltage. This is because thicker dielectric barriers divide a larger proportion of the applied voltage. To avoid the use of unnecessarily larger power supplies, it is clear in Fig. 5(a) that thinner dielectric layers are desirable. Also evident in Fig. 5(a) is that the current dependence of the gas voltage is very similar for all three cases suggesting that the discharge characteristics are altered little by the introduction of dielectric barriers. Around $J_{\rm rms} = 35$ mA/cm$^2$, all three $V_{\rm g}$ curves evolve from a region of positive differential conductivity to a regime of negative differential conductivity. This represents a transition from the $\alpha$ mode to the $\gamma$ mode [11], [18]. Yet, this transition is not seen in the applied voltage curves for which the differential conductivity is always positive. A change in the value of the differential conductivity is however apparent around $J_{\rm rms} = 35$ mA/cm$^2$, particularly for a barrier thickness of $d = 0.5$ and 1 mm. This was also observed experimentally, as shown in Fig. 2.

Phase angle between the current density and the gas voltage is shown in Fig. 5(b) to be similar for all three different barrier thicknesses. On the other hand, the phase angle between the current density and the applied voltage $V_{\rm a}$ is very different among the three different cases. A thicker dielectric barrier introduces a larger series impedance and, therefore, divides

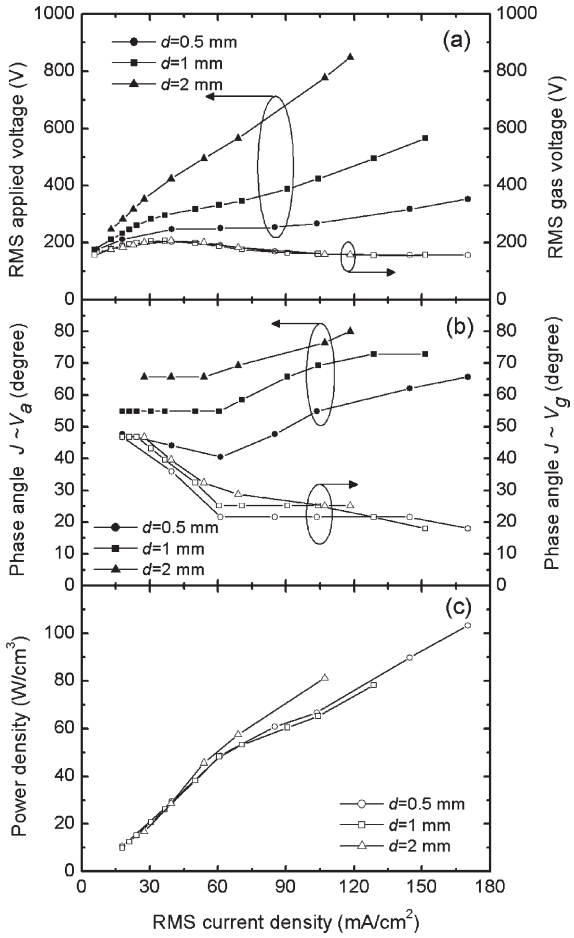


Fig. 5. Current density dependence of (a) the applied and gas voltages, (b) the $J$–$V_{\rm a}$ phase angle and the $J$–$V_{\rm g}$ phase angle, and (c) the dissipated power.

more into the applied voltage. As a result, the electrical characters of the plasma-containing electrode unit are influenced more by the dielectric barrier, and the capacitive nature of the latter increases the $J$–$V_{\rm a}$ phase angle toward 90°. In Fig. 5(c), the dissipated power is shown to follow very similar current dependencies. Given that the dielectric barriers do not consume electrical power, the similarity in the dissipated power suggests that the discharge properties are very similar and relatively unaffected by the introduction of dielectric barriers.

Sheath voltage and sheath thickness are plotted as a function of the current density in Fig. 6. For the three cases of different barrier thicknesses, very similar current dependencies are observed. This suggests that the discharge structure remains very similar. Combining to the results in Fig. 5, it is clear that the electrical and structural characteristics of the gas discharges remain largely unaffected by the presence of dielectric barriers. In addition to the electron trapping mechanism of the RF atmospheric glow discharges [18], the dielectric barriers introduce a new mechanism to limit the current growth. Electrically, they allow for the differential conductivity in the $J$–$V_{\rm a}$ relationship to remain positive in the external circuit while the $J$–$V_{\rm g}$ characteristics are such that the plasma can be operated in the $\gamma$ mode with little danger of plasma instability.

Plasma chemistry at different discharge current densities can be understood by looking at the production of electrons, ions,

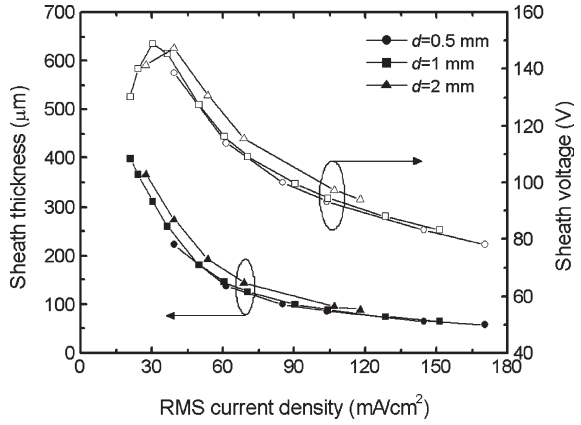


Fig. 6. Current density dependence of sheath voltage and thickness in RF DBD. All conditions are the same as those in Fig. 5.

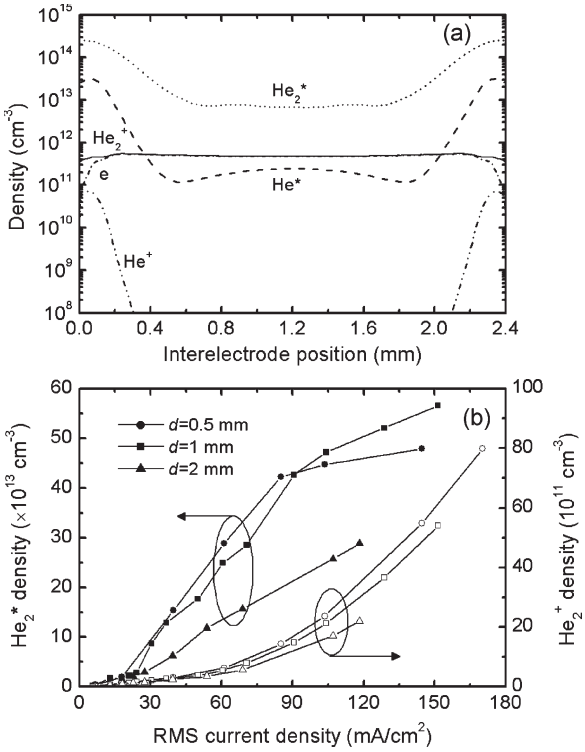


Fig. 7. (a) Spatial distribution of plasma species at $J_{\rm rms} = 60.6$ mA/cm$^2$ and $d = 1$ mm, and (b) current density dependence of $\mathrm{He}_2^*$ and $\mathrm{He}_2^+$.

and helium metastables. Fig. 7(a) shows the spatial distribution of concentrations of electrons, helium ions, and atomic and molecular helium metastables at $J_{\rm rms} = 60.6$ mA/cm$^2$, $f = 13.56$ MHz, and $d = 1$ mm. It is evident that $\mathrm{He}_2^*$ and $\mathrm{He}_2^+$ are the dominant helium metastables and the dominant helium ions, respectively. Molecular helium metastables and ions are known to be the most significant species for ionization and excitation in helium APGD, and as such, they can be used as an indicator of how active the underpinning plasma chemistry may be. As shown in Fig. 7(b), their dependence on the discharge current density is similar, and in general, the densities of $\mathrm{He}_2^*$ and $\mathrm{He}_2^+$ increase with the discharge current. This would suggest a more active plasma chemistry at a large current density; a benefit resulted directly from the introduction of dielectric barriers. It is also worth mentioning some noticeable difference

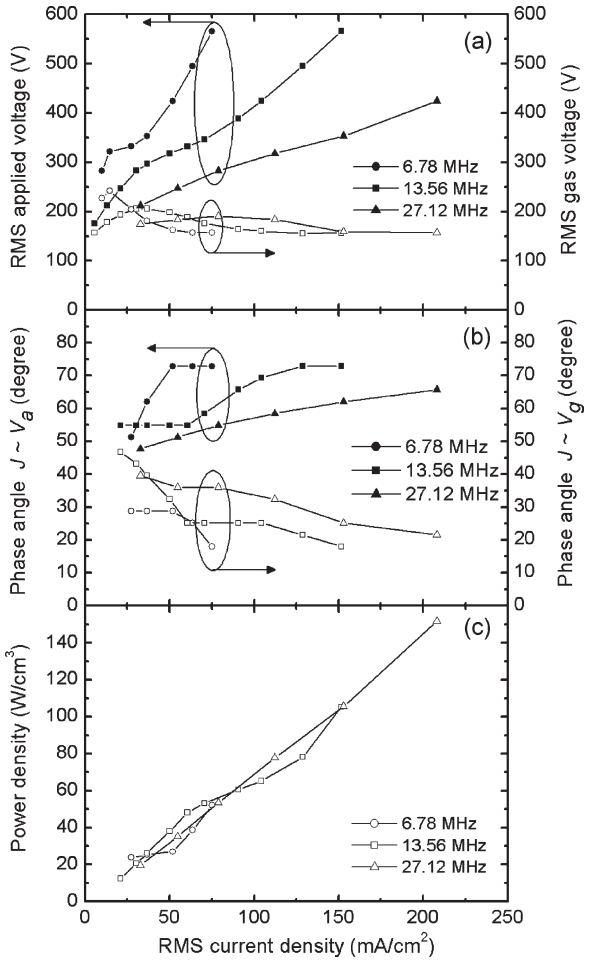


Fig. 8. Current density dependence of (a) the applied and gas voltages, (b) the $J$–$V_{\rm a}$ phase angle and the $J$–$V_{\rm g}$ phase angle, and (c) the dissipated power.

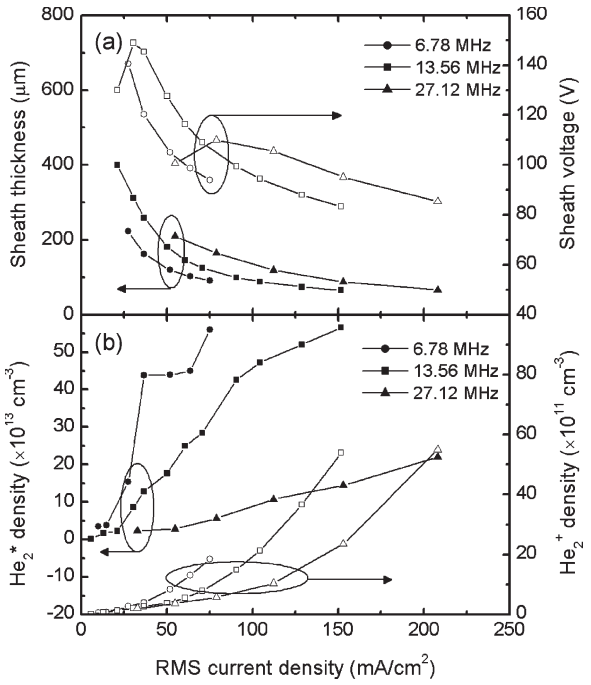


Fig. 9. Current density dependence of (a) sheath voltage and thickness, and (b) molecular helium metastables and ions.

in the three cases in Fig. 7(b). For example, the case of $d = 2$ mm has noticeably lower $\mathrm{He}_2^*$ and $\mathrm{He}_2^+$. This suggests that the barrier thickness introduces a subtle variation in the plasma chemistry even through it does not appear to alter the electrical and structural characters of the discharge. It also suggests that large barrier thicknesses are undesirable because of the less efficient production of the active plasma species.

### *B. Effects of the Excitation Frequency*

Effects of the barrier thickness may be viewed as the effect of the inserted capacitance and, hence, that of the inserted impedance. Since the excitation frequency affects directly the impedance of the dielectric barriers, it is of interest to establish its effect on the RF DBD. For our current study of the effects of the excitation frequency, the barrier thickness is fixed at $d = 1$ mm.

Current dependencies of all electrical parameters are shown in Fig. 8, in which the general trend suggests that the difference is much smaller in the discharge properties than in their behaviors in the external circuit (through $V_{\rm a}$). Larger excitation frequency can extend the operation of the RF DBD into even higher discharge current, as indicated by the fact that the $\alpha$–$\gamma$ mode transition point is at the largest current point in the case of the highest frequency. This is similar to the case of conventional RF APGD and is resulted from a better electron trapping efficiency at larger excitation frequency [20]. It is also worth mentioning that the similarity level in the current dependence of $V_{\rm g}$ and the dissipated power in Fig. 8 is noticeably lower than that in Fig. 5. This suggests that the excitation frequency alters the characteristics of the RF DBD through not only the capacitance of the dielectric barriers but also the underpinning discharge dynamics and structures. The latter has already been established for the RF APGD [20].

Effects of the excitation frequency on the sheath voltage and thickness are shown in Fig. 9(a), suggesting a relatively similar pattern of decreasing sheath voltage and thickness with increasing discharge current. Again, a high excitation frequency is desirable as it allows for plasma operation at large discharge currents. Fig. 9(b) suggests that the $\mathrm{He}_2^+$ concentration at 27.12 MHz can reach $5.7 \times 10^{12}$ cm$^{-3}$ at $J_{\rm rms} = 210$ mA/cm$^2$. This is higher than the maximum $\mathrm{He}_2^+$ concentration achieved at the two lower frequencies, thus suggesting that the high excitation frequency is preferred. On the other hand, it is worth noting that at any given current density, the $\mathrm{He}_2^+$ and $\mathrm{He}_2^*$ concentrations are lower at higher frequencies. This would appear to favor the use of lower excitation frequencies.

Results in Figs. 8 and 9 suggest that the high excitation frequencies are preferred for enhancing the plasma stability, but their benefits for plasma chemistry as indicated by the $\mathrm{He}_2^+$ and $\mathrm{He}_2^*$ production are less obvious. In principle, the use of different excitation frequencies is likely to alter the timescale of plasma dynamics but unlikely to change the timescale of relevant chemical reactions. Therefore, it remains a subject of future studies on how the excitation frequency may be altered to maximize the plasma chemistry even though its effect on plasma stability is now well established and clear. This offers an exciting scope for new APGD physics.

## IV. Conclusion

The challenge of activating the plasma chemistry without compromising the plasma stability is a major issue in APGD science and technology. In this paper, we have analyzed the beneficial effects of introducing the dielectric barriers to radio-frequency atmospheric glow discharges that had hitherto employed bare electrodes. Through a combination of experimental and computational studies, it has been shown that the introduction of dielectric barriers enables much enhanced plasma chemistry without compromising the plasma stability. This is achieved by facilitating a new mechanism to restrict the growth of the discharge current. Despite of a considerable alteration to their signature in the external circuit, the RF DBD have been found to retain very similar electrical and structural characters to the RF APGD. Furthermore, it has been demonstrated that the greatest benefits can be had when the barrier thickness is small or/and the excitation frequency is high. In the broader context of enhancing the plasma chemistry without compromising the plasma stability, dielectric barriers may be considered as an alternative technique for plasma stability control to strategies aimed at exploring and manipulating the spatial [8] and temporal characters [21] of the atmospheric glow discharges.

## References


[1] D. Janasek, J. Franzke, and A. Manz, "Scaling and the design of miniaturized chemical-analysis systems," *Nature*, vol. 442, no. 7101, pp. 374–380, Jul. 2006.

[2] H. Shirai, T. Kobayashi, and Y. Hasegawa, "Synthesis of silicon nanocones using rf microplasma at atmospheric pressure," *Appl. Phys. Lett.*, vol. 87, no. 14, p. 143 112, Oct. 2005.

[3] P. L. Girard-Lauriault, F. Mwale, M. Iordanova, C. Demers, P. Desjardins, and M. R. Wertheimer, "Atmospheric pressure deposition of micropatterned nitrogen-rich plasma-polymer films for tissue engineering," *Plasma Processes Polym.*, vol. 2, no. 3, pp. 263–270, Mar. 2005.

[4] A. Sharma, A. Pruden, Z. Q. Yu, and G. J. Collins, "Bacterial inactivation in open air by the afterglow plume emitted from a grounded hollow slot electrode," *Environ. Sci. Technol.*, vol. 39, no. 1, pp. 339–344, Jan. 2005.

[5] M. Vleugels, G. Shama, X. Deng, E. Greenacre, T. Brocklehurst, and M. G. Kong, "Atmospheric plasma inactivation of biofilm-forming bacteria for food safety control," *IEEE Trans. Plasma Sci.*, vol. 33, no. 2, pp. 824–828, Apr. 2005.

[6] Y. Takao and K. Ono, "A miniature electrothermal thruster using microwave-excited plasmas: A numerical design consideration," *Plasma Sources Sci. Technol.*, vol. 15, no. 2, pp. 211–227, May 2006.

[7] J. G. Eden, "Information display early in the 21st century: Overview of selected emissive display technologies," *Proc. IEEE*, vol. 94, no. 3, pp. 567–574, Mar. 2006.

[8] J. J. Shi and M. G. Kong, "Evolution of discharge structure in capacitive radio-frequency atmospheric microplasmas," *Phys. Rev. Lett.*, vol. 96, no. 10, p. 105 009, Mar. 2006.

[9] U. Kogelschatz, "Filamentary, patterned, and diffuse barrier discharges," *IEEE Trans. Plasma Sci.*, vol. 30, no. 4, pp. 1400–1408, Aug. 2002.

[10] X. H. Yuan and L. L. Raja, "Role of trace impurities in large-volume noble gas atmospheric-pressure glow discharges," *Appl. Phys. Lett.*, vol. 81, no. 5, pp. 814–816, Jul. 2002.

[11] J. J. Shi and M. G. Kong, "Mechanisms of the alpha and gamma modes in radio-frequency atmospheric glow discharges," *J. Appl. Phys.*, vol. 97, no. 2, p. 023 306, Jan. 2005.

[12] S. E. Babayan, G. Ding, G. R. Nowling, X. Yang, and R. F. Hicks, "Characterization of the active species in the afterglow of a nitrogen and helium atmospheric-pressure plasma," *Plasma Chem. Plasma Process.*, vol. 22, no. 2, pp. 255–269, Jun. 2002.

[13] L. Baars-Hibbe, P. Sichler, C. Schrader, C. Gessner, K. H. Gericke, and S. Buttgenbach, "Micro-structured electrode arrays: Atmospheric pressure plasma processes and applications," *Surf. Coat. Technol.*, vol. 174, pp. 519–523, Sep./Oct. 2003.

[14] A. P. Yalin, Z. Q. Yu, O. Stan, K. Hoshimiya, A. Rahman, V. K. Surla, and G. J. Collins, "Electrical and optical emission characteristics of radio-frequency driven hollow slot microplasmas operating in open-air," *Appl. Phys. Lett.*, vol. 83, no. 14, pp. 2766–2768, Oct. 2003.

[15] J. J. Shi, X. T. Deng, R. Hall, J. D. Punnett, and M. G. Kong, "Three modes in a radio frequency atmospheric pressure glow discharge," *J. Appl. Phys.*, vol. 94, no. 10, pp. 6303–6310, Nov. 2003.

[16] S. Y. Moon, J. W. Han, and W. Choe, "Control of radio-frequency atmospheric pressure argon plasma characteristics by helium gas mixing," *Phys. Plasmas*, vol. 13, no. 1, p. 013 504, Jan. 2006.

[17] J. J. Shi, D. W. Liu, and M. G. Kong, "Plasma stability control using dielectric barriers in radio-frequency atmospheric-pressure glow discharges," *Appl. Phys. Lett.*, vol. 89, no. 8, p. 081 502, Aug. 2006.

[18] J. J. Shi and M. G. Kong, "Mode characteristics of radio-frequency atmospheric glow discharges," *IEEE Trans. Plasma Sci.*, vol. 33, no. 2, pp. 624–630, Apr. 2005.

[19] X. T. Deng, J. J. Shi, and M. G. Kong, "Physical mechanisms of inactivation of *Bacillus subtilis* spores using cold atmospheric plasmas," *IEEE Trans. Plasma Sci.*, vol. 34, no. 4, pp. 1310–1316, Aug. 2006.

[20] J. J. Shi and M. G. Kong, "Expansion of the plasma stability range in radio-frequency atmospheric-pressure glow discharges," *Appl. Phys. Lett.*, vol. 87, no. 20, p. 201 501, Nov. 2005.

[21] M. G. Kong and X. T. Deng, "Electrically efficient production of a diffuse nonthermal atmospheric plasma," *IEEE Trans. Plasma Sci.*, vol. 31, no. 4, pp. 7–18, Feb. 2003.


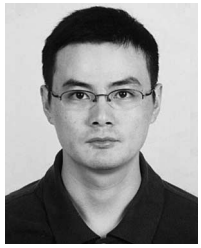

**Jianjun J. Shi** received the B.Sc. and M.Sc. degrees in physics both from Nanjing University, Nanjing City, China, in 1999 and 2002, respectively, and the Ph.D. degree in electrical engineering from Loughborough University, Leicestershire, U.K., in 2005.

He is currently a Postdoctoral Scientist with the Plasma and Pulsed Power Group ($P^3G$), Loughborough University. His research interests include atmospheric pressure glow discharges and their biomedical applications.

Dr. Shi won an IEEE NSPP Graduate Scholarship Award in 2005.

**Dawei W. Liu** received the B.Sc. degree from China University of Geosciences, Wuhan City, China, in 2002, and the M.Sc. degree from Loughborough University, Leicestershire, U.K., in 2005, both in electronics engineering. Since October 2005, he has been working toward the Ph.D. degree in the Plasma and Pulsed Power Group ($P^3G$) at Loughborough University.

His current research interests include experimental and computational studies of RF APGDs.

**Michael G. Kong** (M'94–SM'98) received the B.Sc. and M.Sc. degrees in electronics engineering from Zhejiang University, Hangzhou, China, in 1984 and 1987, respectively, and the Ph.D. degree in electrical engineering from Liverpool University, Liverpool, U.K., in 1992.

After his research and faculty positions with the Liverpool and Nottingham Universities, U.K., he joined Loughborough University, Leicestershire, U.K., in 1999, where he currently holds a Chair in bioelectrical engineering and leads the Plasma and Pulsed Power Group ($P^3G$). At Loughborough University, he is also the Head of Energy Research Division whose research encompasses gas plasmas, pulsed power, and renewable energy. His current research interests include atmospheric pressure glow discharges, high-intensity ultrashort electric pulses, and their biomedical applications. In these areas and others, he has published 180 papers in scientific journals and some peer-reviewed conference proceedings.

Dr. Kong was a Guest Editor for a Special Issue of the IEEE Transactions on Plasma Science on Nonthermal Medical/Biological Applications of Ionized Gases and Electromagnetic Fields (August 2006). He is a member of the Editorial Board of Plasma Sources Science and Technology.